Causality and intrinsic thermoacoustic instability modes

Emilien Courtine, Laurent Selle, Franck Nicoud, Wolfgang Polifke, Camilo Silva, Michaël Bauerheim, Thierry Poinsot

Causality and intrinsic thermoacoustic instability modes

By E. Courtine†, L. Selle†, F. Nicoud‡, W. Polifke¶, C. Silva¶, M. Bauerheim‖ AND T. Poinsot†

Direct numerical simulation of a confined laminar premixed flame has been performed in an anechoic combustor, showing self-sustained intrinsic thermoacoustic oscillations. Theoretical predictions based on acoustic jump relations and the $n-\tau$ model for the flame are presented and causality concerns are discussed. The instability's frequency and mode structure are recovered numerically with very good accuracy. A detailed discussion on the interplay of the physical phenomena responsible for this dynamical coupling is also carried out.

1. Introduction

Combustion instabilities are a major problem for many industrial programs (Krebs *et al.* 2002; Lieuwen & Yang 2005) and a central research topic in multiple groups today because their impact on combustion chambers is both large and difficult to predict. Even though brute force LES has shown its potential in this field (Moin & Apte 2006; Mahesh *et al.* 2006; Schmitt *et al.* 2007; Staffelbach *et al.* 2009; Wolf *et al.* 2009), the need to understand combustion instabilities and not only to reproduce them in a simulation has led to the development of other tools. The workhorse of such approaches is Helmholtz codes where the mean flow is frozen and only the wave equation in a reacting flow is solved (Nicoud *et al.* 2007). In these formulations, flames are replaced by active acoustic elements. The acoustic emission of these elements is due to dilatation induced by the unsteady reaction rate q' and is presumed to depend only on the acoustic velocity upstream of the flame (Poinsot & Veynante 2011) through a function called Flame Transfer Function (FTF).

The FTF paradigm was first introduced by Crocco (Crocco 1965), who expressed the unsteady reaction rate q' of a flame as a function of the upstream acoustic velocity u' at a reference point P, usually located in the inlet duct, close to the chamber (Truffin & Poinsot 2005) (all fluctuating quantities are written as $f' = \Re(\hat{f}e^{-j\omega t})$)

$$q' = \frac{\rho_1 c_1^2}{\gamma - 1} S_1 n u'(t-\tau) \quad \text{or} \quad \hat{q} = \frac{\rho_1 c_1^2}{\gamma - 1} S_1 n \hat{u} e^{j\omega\tau} \ , \tag{1.1}$$

where ρ_1 and c_1 correspond to the density and sound speed of the fresh gases, and S_1 is the section of the upstream duct (Figure 1). The parameters n and τ are the interaction index and the flame delay of the FTF, respectively. FTFs are global functions which include all mechanisms controlling the flame response (e.g., vortex formation caused by

† IMF Toulouse, INP de Toulouse and CNRS, France
‡ Université Montpellier 2, France
¶ Fachgebiet für Thermodynamik, TU München, Germany
‖ CERFACS, France

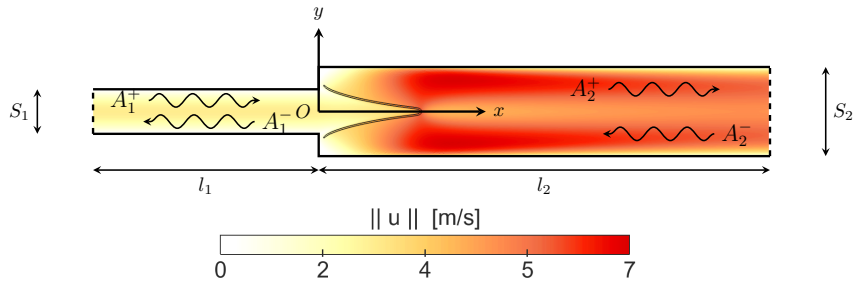

FIGURE 1. An illustration of wave propagation in a laminar combustor. The A_1^- and A_2^+ waves are not expected to influence the unsteady reaction for causality reasons. Colors correspond to the mean axial velocity field. The flame position is indicated by the black isocontour.

the acoustic velocity surge, vortex convection followed by vortex combustion). Recently, a normalized FTF formulation has been preferred by most authors

$$\frac{\hat{q}}{\bar{q}} = F\frac{\hat{u}}{\bar{u}} \ , \tag{1.2}$$

where the bar denotes time average. The F function is directly linked to n and τ: it is simple to show that $\theta F = ne^{j\omega\tau}$ where $\theta = T_2/T_1 - 1$ and T_2 is the adiabatic flame temperature while T_1 is the fresh gases temperature. In general, F (or n and τ) are functions of the forcing frequency. In recent theories, F is also a function of the forcing amplitude (Palies *et al.* 2011*b*). Equation (1.1) defines a Flame Tranfer Function between u' and q' when it does not depend on amplitude, or a Flame Describing Function (FDF) when it also depends on the amplitude of the fluctuations (Noiray *et al.* 2008). The present analysis is limited to the linear framework of FTFs even though the flame DNS presented in the following sections obviously captures both linear and non-linear effects.

While the FTF and FDF paradigms have been used in numerous approaches, they have an intriguing property linked to causality: expressing the unsteady reaction rate q' as a function of the velocity fluctuations upstream of the combustor u' seems a plausible method, because the combustor inlet velocity certainly affects the combustor unsteady reaction rate. This question, however, may also be considered from an acoustic point of view, as sketched in Figure 1. In a combustion chamber, assuming one-dimensional acoustic wave propagation, the velocity and pressure perturbations at each point of a duct (numbered $i = 1$ to 2, $x = 0$ corresponds to the flame position) can be written as

$$u_i'(x,t) = \left[A_i^+ e^{jkx} - A_i^- e^{-jkx}\right] e^{-j\omega t} \tag{1.3}$$

$$p_i'(x,t) = \rho_i c_i \left[A_i^+ e^{jkx} + A_i^- e^{-jkx}\right] e^{-j\omega t} \ . \tag{1.4}$$

If one considers the inlet duct (index 1), the quantity that affects combustion is the wave propagating from the inlet duct towards the chamber A_1^+. The wave leaving the chamber to propagate upstream (A_1^-) should not be able to modify the combustion in the chamber for simple causality reasons: it is going in the wrong direction. In the standard FTF model (Eq. 1.1), the quantity controlling q' is presumed to be the velocity fluctuations at a reference point P located in the inlet duct and close from the rim

$$u'(P,t) = u'(x=0,t) = (A_1^+ - A_1^-)e^{-j\omega t} \ . \tag{1.5}$$

Therefore $u'(P,t)$ contains one piece of information (A_1^-) that has the right causality link with q' and one that has the wrong causality link (A_1^+). A wave propagating upstream and away from the flame cannot affect the unsteady reaction rate so its contribution

should not be included in an FTF model. This argument is often used to justify the use of scattering matrices in network models for combustion instabilities: scattering matrices link outgoing waves (A_1^-, A_2^+) to ingoing waves (A_1^+, A_2^-) so that causality is naturally satistied (Paschereit *et al.* 2002). An acoustically causal alternative to Crocco's model would be to link q' with the two waves propagating towards the flame (A_1^+, A_2^-).

Despite this apparent flaw in the construction of FTF and FDF models, Crocco-type FTF approaches have been widely used in the past and have produced successful results in multiple cases (Krueger *et al.* 2000; Nicoud *et al.* 2007; Motheau *et al.* 2013; Hoeijmakers *et al.* 2014). Moreover, the argument used in the previous paragraph to disqualify the classical Crocco model may be too simple: there are mechanisms such as mode conversion (Schadow & Gutmark 1992; Komarek & Polifke 2010; Palies *et al.* 2011*a*; Scarpato *et al.* 2013; Kim & Santavicca 2013) where an acoustic wave, even if it propagates upstream, can be converted into a vortical wave when it hits an obstacle or a flame holder, for example. Such mechanisms open the possibility that certain waves propagating upstream and apparently unable to affect the flame any more, can indeed convert into a convective wave which propagates downstream and modifies the combustion process.

If Crocco's model is valid, then a new class of instabilities must exist: Intrinsic Thermo Acoustic (ITA) modes. ITA modes should appear even in a perfectly anechoic system (i.e., where the incoming waves A_1^+ and A_2^- vanish). This was proven by the Eindhoven (Hoeijmakers *et al.* 2014) and Munich (Emmert *et al.* 2014) groups and the demonstration can be quite simple, as indicated below†. Assume that Crocco's model is valid and consider the geometry of Figure 1, where both inlet and outlet are fully anechoic, so the incoming waves vanish: $A_1^+ = A_2^- = 0$. The jump conditions at the flame (assumed to be compact) are the continuity of pressure and a jump of acoustic velocity due to heat release and area change (Dowling 1995; Poinsot & Veynante 2011; Bauerheim *et al.* 2014)

$$p_2'(x=0,t) = p_1'(x=0,t) \qquad \text{and} \qquad \mathrm{S_2 u_2'(x=0,t) = S_1 u_1'(x=0,t)(1+n e^{j\omega\tau})} \ , \quad (1.6)$$

where the $n-\tau$ formulation has been used to express the unsteady heat release q'. If $A_1^+ = A_2^- = 0$, using Eqs. (1.3) and (1.4), Eq. (1.6) becomes

$$\rho_2 c_2 A_2^+ = \rho_1 c_1 A_1^- \qquad \text{and} \qquad \mathrm{S_2 A_2^+ = -S_1 A_1^- (1+n e^{j\omega\tau})} \ , \quad (1.7)$$

which leads to

$$1 + \Gamma(1 + n e^{j\omega\tau}) = 0 \ , \quad (1.8)$$

where $\Gamma = (S_1\rho_2 c_2)/(S_2\rho_1 c_1)$ depends only on the section change and the variation of thermodynamic variables between cold and burnt gas. Equation (1.8) has no trivial solution in the general case when τ is a function of ω. However, if τ is assumed to be independent of ω, which is a reasonable assumption for many flames (Durox *et al.* 2009), Eq. (1.8) has simple solutions that provide the real (frequency) and imaginary (growth rate) parts of any mode ω. Here we only consider the first mode with lowest frequency

$$\omega_r = \frac{\pi}{\tau} \qquad \text{so that} \qquad T = 2\tau \ , \quad (1.9)$$

where $T = 2\pi/\omega_r$ is the mode period. The corresponding growth rate is given by

$$\omega_i = \frac{1}{\tau} \ln\left(\frac{n\Gamma}{\Gamma+1}\right) \ . \quad (1.10)$$

† The present demonstration is limited to the simplest case. Readers are referred to the PhD thesis of Hoeijmakers (2014) for a thorough description of the mathematical methodologies needed to study the dispersion equations of thermoacoustic modes for 1D compact flames.

This mode is unusual in thermoacoustics: it is obtained in a situation where acoustic losses at the burner's ends are maximum (anechoic terminations). The period of the first ITA mode is twice the flame delay and is not linked to any acoustic mode of the duct. Note that no acoustic mode can exist here because both terminations are anechoic, therefore the only time scale in this problem is the flame delay τ. For this mode, Eq. (1.1) shows that q' will be out of phase with the reference velocity upstream of the flame, which implies that q' will be in phase with pressure perturbations since p' and u' have opposite phases in the inlet duct ($A_1^+ = 0 \implies u'_1 + p'_1/(\rho_1 c_1) = 0$) (see Figure 2). Moreover, this mode is amplified for any flame delay τ but only if the interaction index n is larger than a critical threshold n_c given by‡

$$\omega_i \ > \ 0 \qquad \Longleftrightarrow \qquad n \ > \ n_c = \frac{\Gamma + 1}{\Gamma} \ . \tag{1.11}$$

Note that this criterion may also be found via a simple acoustic energy budget. Each anechoic termination does indeed lose an acoustic flux $\mathcal{F}_i = 1/2 \ |\hat{p}_i|^2 S_i/(\rho_i c_i)$, while the source term created by the flame for this mode is $\mathcal{R} = n/2 \ |\hat{p}_1|^2 S_1(\rho_1 c_1)$. The Rayleigh criterion for instability writes $\mathcal{R} > \mathcal{F}_1 + \mathcal{F}_2$, which can be rearranged to yield criterion (1.11) on n, recalling that $\Gamma = (S_1\rho_2 c_2)/(S_2\rho_1 c_1)$. In terms of FTF, the instability starts when F exceeds a critical threshold F_c deduced from Eq. (1.11)

$$|F| > F_c \qquad \text{with} \qquad \mathrm{F_c} = \frac{\Gamma + 1}{\Gamma\theta} \ . \tag{1.12}$$

For a perfect gas, $\Gamma = S_1/S_2\sqrt{T_1/T_2}$ so that the threshold F_c can be written as

$$F_c = \frac{1}{T_2/T_1 - 1}\left(1 + \frac{S_2}{S_1}\sqrt{\frac{T_2}{T_1}}\right) \ . \tag{1.13}$$

Equation (1.13) shows that the ITA stability threshold goes down when the section ratio between inlet duct and combustion chamber goes down (S_2/S_1 decreasing) or when the temperature ratio goes up (T_2/T_1 increasing): intense flames in chambers with small section changes (strong confinement) should be more prone to intrinsic instabilities. Should Crocco's model hold, intrinsic instabilities would appear for these flames as long as $F > F_c$, even if both ends of the system are anechoic.

Using previous derivations, Eqs (1.6), (1.7), and (1.9) are used to derive the spatial structure of the intrinsic thermoacoustic mode, Eq. (1.14), which is shown on Figure 2.

$$\left\{\begin{array}{rcl} \dfrac{|\hat{p}_2|}{|\hat{p}_1|} & = & 1 \\ \dfrac{|\hat{u}_2|}{|\hat{u}_1|} & = & \dfrac{S_1}{S_2}\left(\theta|F| - 1\right) \end{array}\right. \qquad \left\{\begin{array}{rcl} \arg[\hat{p}_1] & = & -\dfrac{\pi}{c_1\tau}x \\ \arg[\hat{u}_1] & = & -\dfrac{\pi}{c_1\tau}x \end{array}\right. \qquad \left\{\begin{array}{rcl} \arg[\hat{p}_2] & = & \dfrac{\pi}{c_2\tau}x \\ \arg[\hat{u}_2] & = & \dfrac{\pi}{c_2\tau}x + \pi \end{array}\right. \tag{1.14}$$

In the next section, the validity of Crocco's formulation, Eq. (1.1), will be checked on a laminar flame. Intrinsic modes revealed by DNS will be presented in Section 3.

‡ In usual thermoacoustic modes, stability is first determined by the delay τ that must be in a certain range to guarantee stability. n plays no role when acoustic losses are not accounted for.

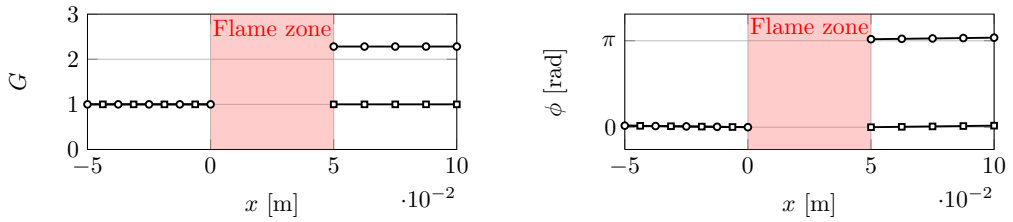

FIGURE 2. Theoretical structure of an ITA mode: pressure (—□—) and velocity (—○—). Left: modulus. Right: phase.

2. Verifying Crocco's model

In a first step, Crocco's relation (1.1) was checked by forcing a laminar flame from either the upstream ($A_1^+ = Ae^{-j\omega t}$) or the downstream end ($A_2^- = Ae^{-j\omega t}$) in two different simulations, leading to the same velocity fluctuations at the reference point $u'(P,t)$ but different systems of waves ($A_i^\pm$) (Truffin & Poinsot 2005).

The configuration corresponds to a laminar dihedral flame previously studied by Mejia *et al.* (2014) and Selle *et al.* (2011) on which a combustion chamber has been added for the simulation of ITA modes (Figure 1). The width of the inlet duct $S_1 = 1$ cm is fixed, while the width of the combustion chamber can be adjusted in the DNS. A homogeneous methane-air mixture at 300 K and equivalence ratio 0.95 is fed through the inlet duct at 1.8 m/s, leading to a Reynolds number $\mathrm{Re}_1 \simeq 2000$. The DNS code used for the acoustic forcing simulations is AVBP. Chemistry is modeled using a two-step chemical scheme for methane-air flames. A high-order fully explicit scheme is used to advance the compressible reacting Navier-Stokes equations. Acoustic boundary conditions at the inlet and outlet of the combustor are treated using the NSCBC method (Poinsot & Lele 1992; Granet *et al.* 2010). For all present simulations, fully non-reflecting conditions are used to allow ITA modes to develop. The geometry (ratio $S_2/S_1 = 6$) and the temperature jump ($T_2/T_1 = 7.3$) correspond to a case where the critical gain is $F_c = 2.7$ (see Eq. (1.13)). When the FTF of this flame is measured, its values are of order unity, hence always smaller than F_c. Therefore no intrinsic instability is expected in this configuration†.

Acoustic excitation is added by forcing the acoustic waves entering the inlet (A_1^+) or the outlet (A_2^-). Both harmonic forcing and impulse excitations were used to reconstruct the FTF, leading to the same result.

Results presented on Figure 3 show that the FTF between the velocity at the reference point and the integrated unsteady heat release rate is independent of the side from which acoustic waves are introduced in the combustor. For reference, the measurements of Mejia *et al.* (2014) are added even though they were performed without confinement (free flame without combustion chamber). This verification of Crocco's model does not prove that it is always valid, but it was sufficiently conclusive to try to capture intrinsic modes on this flame, as described in the next section.

3. Capturing an ITA mode

Since Crocco's relation seems to hold for the present flame, intrinsic modes should appear if parameters of the flame are chosen so that $F > F_c$. To destabilize an ITA

† Note that the measurement of the FTF of the flame in an anechoic test rig would be impossible if it were intrinsically unstable, except at the frequency at which it resonates.

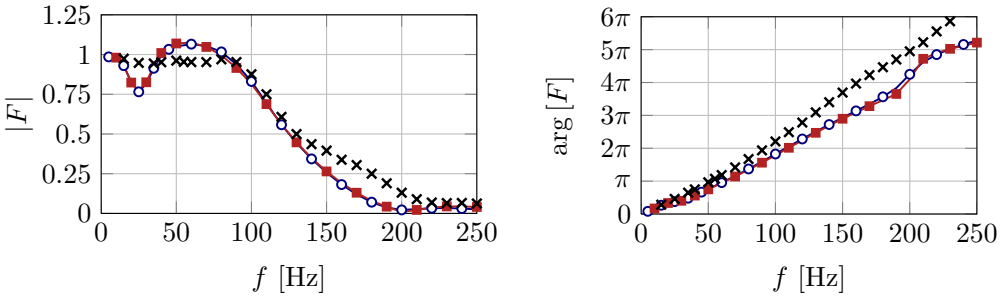

FIGURE 3. FTFs of the flame of Figure 1 for a confinement corresponding to $S_2/S_1 = 6$. DNS using upstream forcing (—○—) and downstream forcing (—■—), and experimental results using upstream forcing for the unconfined flame (×). From left to right: modulus and argument of F against forcing frequency. The reference point P is located upstream from the dump plane.

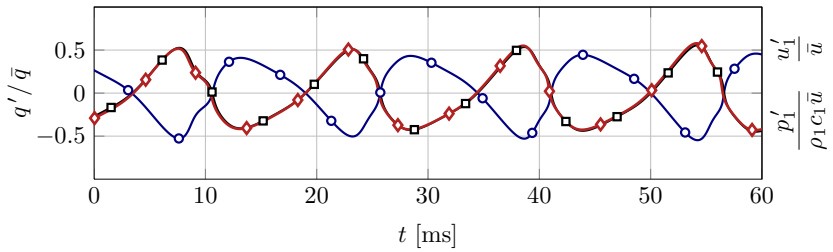

FIGURE 4. Time evolutions of global heat release (—◇—), pressure (—□—), and velocity (—○—) at a reference point located upstream from the dump plane, from DNS with $S_2/S_1 = 2$.

mode, the critical threshold had to be lowered: this was achieved by diminishing the section change S_2/S_1 from 6 to 2. All other parameters (flow rates and equivalence ratio) were unchanged, and we also supposed that the FTF remained unchanged for the purpose of the analysis. For this case, the critical value for instability is $F_c = 1.01$ so that there is a range of frequency where $F > F_c$, which is $[40; 80]$ Hz (Figure 3). This configuration proved to be extremely unstable as shown by the time traces of pressure, heat release, and velocity signals displayed in Figure 4. Right from the initial condition, the flame entered a strong oscillation at a frequency of 62 Hz (period: $T = 16$ ms), which is indeed in the range of frequencies where $F > F_c$. At this frequency, the phase of the FTF of Figure 3 is close to π, and τ close to 8 ms. This is consistent with the theoretical evaluation of Eq. (1.9), which states that the period T must be equal to twice the flame delay τ. Also, Figure 4 shows that q' and p' are exactly in phase, as predicted by the theory.

Note that Figure 4 displays non-harmonic fluctuations of high and constant amplitude, suggesting that the mode has entered a limit-cycle. Although oscillation amplitudes are high and beyond the limit of the linear regime, the DNS matches theoretical predictions.

To check whether the mode observed in this DNS is indeed an ITA mode, the mode structure obtained by DNS was compared to the theoretical model (Figure 2) in terms of modulus and phase of the velocity perturbations measured at various points in the inlet to the outlet of the combustor. Figure 5 shows that the phase, as well as the modulus, of velocity perturbations predicted by the theoretical model of Eq. (1.6) are very well recovered in the DNS. The 1D compact acoustic theory is not plotted in the flame zone. Agreement is good on both sides of the flame: the ratio between the modulus of acoustic velocity perturbations upstream and downstream of the flame is recovered by the DNS.

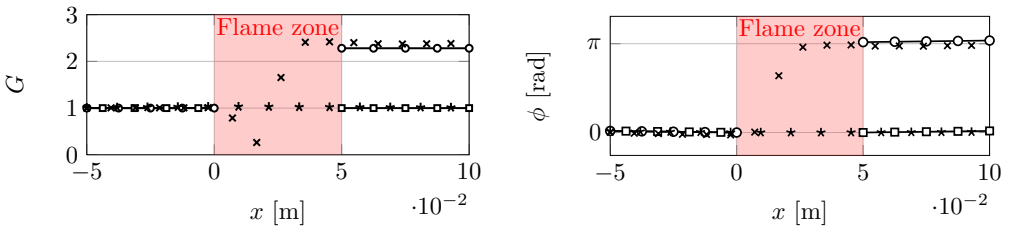

FIGURE 5. Spatial structure of an ITA mode. Comparison between theory: pressure (—□—) and velocity (—○—), and DNS: pressure (*) and velocity (×). Left: modulus. Right: phase.

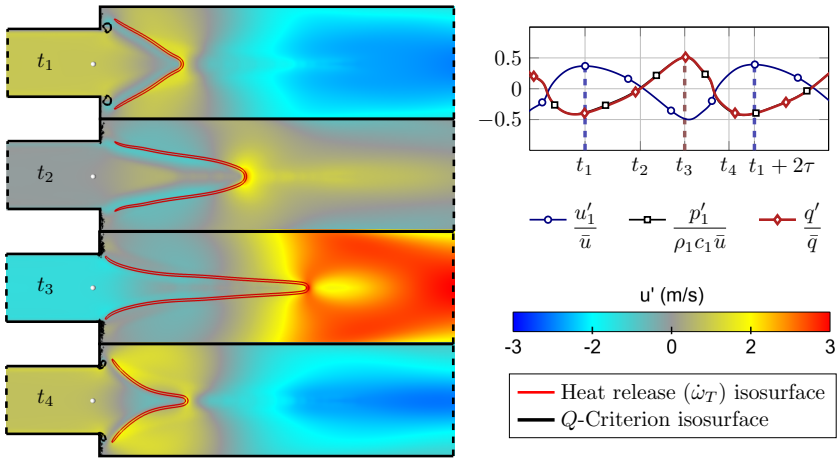

FIGURE 6. One cycle of the ITA mode. The black isoline corresponds to a high value of the Q criterion and marks intense vortices. The heat release rate is indicated by red iso lines. The background color corresponds to the axial velocity field.

The π phase shift for the acoustic velocity is also obtained in the DNS, suggesting that the captured mode is indeed the intrinsic mode predicted theoretically.

4. ITA analysis: mode conversion and kinematic over-restoration

The final part of this work is devoted to the analysis of the scenario of the ITA mode revealed by the DNS. Indeed, at this point, even though the structure revealed by the DNS matches theoretical predictions, the question of causality remains unexplained. This section shows that mode conversion, i.e., the transformation of an acoustic wave into a convective wave is the mechanism that must be introduced into the analysis to understand the instability loop and explain the apparent causality paradox. In the present case the transformation takes place at the sharp corner, where vorticity is generated and where the flame is anchored. The second mechanism needed to elucidate the ITA is Kinematic Over-Restoration (KOR), which controls the second part of the instability loop. To gain more insight into these mechanisms, a complete ITA cycle was analyzed using DNS data. Figure 6 shows four snapshots of the flame position during one cycle. The time evolution of the reference acoustic velocity and pressure in the chamber are plotted on the right hand-side of the figure.

The cycle can be described as follows: assume that a pair of vortices is created on both sides of the flame at $t = t_1$ when the acoustic velocity is maximal at the dump plane.

These vortices push the flame anchoring point apart and a convective perturbation then propagates along the flame front (instant t_2). This perturbation takes a time τ before the flame reaches its maximum elongation and heat release rate is maximum at time t_3. Kinematic Over-Restoration subsequently takes place. Standard kinematic restoration happens when a flame, pushed away from its stable position, naturally reverts to steady state. Here, not only is the flame far from its equilibrium position, but the inlet velocity is also minimal: these two combined factors lead to very fast contraction of the flame. This is why the unsteady reaction rate becomes negative at time t_4. Strong contraction of the flame results in negative dilatation and acoustic pressure, which in turns induces a velocity surge upstream from the flame. This positive inlet acoustic velocity again initiates mode conversion at the corner and creates a new pair of vortices, thereby closing the unstable loop. In this scenario, acoustics plays a role only between instants t_3 and t_4 to trigger a pair of vortices through mode conversion at the corner. No acoustic mode of the full system is involved.

This scenario corresponds to the DNS observations and matches theoretical predictions. Furthermore, it explains why causality is actually satisfied. The velocity signal measured in the inlet duct upstream from the rim is not the cause of vortex formation but it is synchronous with it: at time t_4, the acoustic wave propagating upstream from the chamber to the inlet duct touches the corner and mode conversion begins. A few microseconds later, the upstream acoustic wave continues to propagate upstream from the dump plane and appears in the reference velocity signal, but it plays no further role as it keeps propagating away from the flame.

5. Conclusion

The starting point of this study is an apparent break of causality of the classical Crocco's model for flame-acoustic coupling which leads to the existence of intrinsic thermoacoustic modes (ITA) in an anechoic environment. Here a perfectly premixed flame was studied using DNS. Crocco's model was first verified by forcing a laminar flame from upstream and downstream boundary conditions and showing that the transfer function between u' at a reference point and the unsteady reaction rate q' was the same. DNS also revealed that apparent causality issues were due to mode conversion in the plane separating the inlet duct and the combustion chamber.

As suggested by Bomberg *et al.* (2014), Emmert *et al.* (2014), and Hoeijmakers *et al.* (2014), the validity of Crocco's model implies that a new class of thermoacoustic modes (called ITA for Intrisic ThermoAcoustic) must exist. In these modes, no coupling with the acoustic modes of the chamber or the inlet duct is required. ITA modes can develop in perfectly anechoic systems, and a 2D DNS of a laminar flame was used to exhibit such a mode. Its structure was analyzed and shown to match the theoretical prediction. Mode conversion at the dump plane corner and KOR (kinematic over-restoration) were shown to be the two mechanisms controlling the ITA unstable loop.

This work opens multiple new paths for thermoacoustics: (1) it shows that intrinsic modes may have appeared in multiple other systems but were ignored up to now†, (2) it demonstrates that the robustness of a combustor may be assessed by testing its response to waves propagating upstream from the chamber to the inlet to see how strong mode conversion is at the chamber inlet.

† The signature of these modes would be that their frequencies do not match any eigenmode of the combustor.

Acknowledgments

We acknowledge the support of the European commission through the ERC advanced grant INTECOCIS GA 319067. This work was also granted access to the high-performance computing resources of CINES under the allocation x20142b7036 made by GENCI.

REFERENCES

Bauerheim, M., Nicoud, F. & Poinsot, T. 2014 Theoretical analysis of the mass balance equation through a flame at zero and non-zero Mach numbers. *Combust. Flame* **162**, 60–67.

Bomberg, S., Emmert, T. & Polifke, W. 2014 Thermal Versus Acoustic Response of Velocity Sensitive Premixed Flames. In *35th Symp. (Int.) on Combustion*. San Francisco, CA, USA.

Crocco, L. 1965 Theoretical studies on liquid propellant rocket instability. In *10th Symp. (Int.) on Combustion*, pp. 1101–1128. Pittsburgh PA, USA.

Dowling, A. P. 1995 The calculation of thermoacoustic oscillations. *J. Sound Vib.* **180**, 557–581.

Durox, D., Schuller, T., Noiray, N. & Candel, S. 2009 Experimental analysis of nonlinear flame transfer functions for different flame geometries. *Proc. Combust. Inst.* **32**, 1391–1398.

Emmert, T., Bomberg, S. & Polifke, W. 2014 Intrinsic thermoacoustic instability of premixed flames. *Combust. Flame* **162**, 75–85.

Granet, V., Vermorel, O., Leonard, T., Gicquel, L., & Poinsot, T. 2010 Comparison of nonreflecting outlet boundary conditions for compressible solvers on unstructured grids. *AIAA J.* **48**, 2348–2364.

Hoeijmakers, M. 2014 Flame-acoustic coupling in combustion instabilities. PhD thesis, T.U. Eindhoven.

Hoeijmakers, M., Kornilov, V., Lopez Arteaga, I., de Goey, P. & Nijmeijer, H. 2014 Intrinsic instability of flame-acoustic coupling. *Combust. Flame* **161**, 2860–2867.

Kim, K. & Santavicca, D. 2013 Interference mechanisms of acoustic/convective disturbances in a swirl-stabilized lean-premixed combustor. *Combust. Flame* **160**, 1441–1457.

Komarek, T. & Polifke, W. 2010 Impact of swirl fluctuations on the flame response of a perfectly premixed swirl burner. *J. Eng. Gas Turb. Power* **132**, 061503.

Krebs, W., Flohr, P., Prade, B. & Hoffmann, S. 2002 Thermoacoustic stability chart for high intense gas turbine combustion systems. *Combust. Sci. Tech.* **174**, 99–128.

Krueger, U., Hueren, J., Hoffmann, S., Krebs, W., Flohr, P. & Bohn, D. 2000 Prediction and measurement of thermoacoustic improvements in gas turbines with annular combustion systems. In *ASME Turbo Expo*. Munich, Germany.

Lieuwen, T. & Yang, V. 2005 Combustion Instabilities in Gas Turbine Engines: Operational Experience, Fundamental Mechanisms and Modeling. *Prog. Astronaut. Aeronaut. AIAA* Vol. 210.

Mahesh, K., Constantinescu, G., Apte, S., Iaccarino, G., Ham, F. & Moin, P. 2006 Large eddy simulation of reacting turbulent flows in complex geometries. *ASME J. Appl. Mech.* **73**, 374–381.

Mejia, D., Selle, L., Bazile, R. & Poinsot, T. 2014 Wall-temperature effects on flame response to acoustic oscillations. In *35th International Symposium on Combustion*. San Francisco, CA, USA.

Moin, P. & Apte, S. V. 2006 Large-eddy simulation of realistic gas turbine combustors. *AIAA J.* **44**, 698–708.

Motheau, E., Selle, L. & Nicoud, F. 2013 Accounting for convective effects in zero-Mach-number thermoacoustic models. *J. Sound Vib.* **333**, 246–262.

Nicoud, F., Benoit, L., Sensiau, C. & Poinsot, T. 2007 Acoustic modes in combustors with complex impedances and multidimensional active flames. *AIAA J.* **45**, 426–441.

Noiray, N., Durox, D., Schuller, T. & Candel, S. 2008 A unified framework for nonlinear combustion instability analysis based on the flame describing function. *J. Fluid Mech.* **615**, 139–167.

Palies, P., Durox, D., Schuller, T. & Candel, S. 2011*a* Experimental study on the effect of swirler geometry and swirl number on flame describing functions. *Combust. Sci. Tech.* **183**, 704–717.

Palies, P., Durox, D., Schuller, T. & Candel, S. 2011*b* Nonlinear combustion instability analysis based on the flame describing function applied to turbulent premixed swirling flames. *Combust. Flame* **158**, 1980 – 1991.

Paschereit, C. O., Polifke, W., Schuermans, B. & Mattson, O. 2002 Measurement of transfer matrices and source terms of premixed flames. *J. Eng. Gas. Turb. Power* **124**, 239–247.

Poinsot, T. & Lele, S. 1992 Boundary conditions for direct simulations of compressible viscous flows. *J. Comput. Phys.* **101**, 104–129.

Poinsot, T. & Veynante, D. 2011 *Theoretical and Numerical Combustion*. Third Edition (www.cerfacs.fr/elearning).

Scarpato, A., Ducruix, S. & Schuller, T. 2013 Optimal and off-design operations of acoustic dampers using perforated plates backed by a cavity. *J. Sound Vib.* **332**, 4856–4875.

Schadow, K. & Gutmark, E. 1992 Combustion instability related to vortex shedding in dump combustors and their passive control. *Prog. Energy Combust. Sci.* **18**, 117–132.

Schmitt, P., Poinsot, T., Schuermans, B. & Geigle, K. P. 2007 Large-eddy simulation and experimental study of heat transfer, nitric oxide emissions and combustion instability in a swirled turbulent high-pressure burner. *J. Fluid Mech.* **570**, 17–46.

Selle, L., Poinsot, T. & Ferret, B. 2011 Experimental and numerical study of the accuracy of flame-speed measurements for methane/air combustion in a slot burner. *Combust. Flame* **158**, 146–154.

Staffelbach, G., Gicquel, L., Boudier, G. & Poinsot, T. 2009 Large eddy simulation of self-excited azimuthal modes in annular combustors. *Proc. Combust. Inst.* **32**, 2909–2916.

Truffin, K. & Poinsot, T. 2005 Comparison and extension of methods for acoustic identification of burners. *Combust. Flame* **142**, 388–400.

Wolf, P., Staffelbach, G., Roux, A., Gicquel, L., Poinsot, T. & Moureau, V. 2009 Massively parallel LES of azimuthal thermo-acoustic instabilities in annular gas turbines. *C. R. Acad. Sci. Mécanique* **337**, 385–394.